

SURVIVABILITY AND GROUND RISK POTENTIAL OF SCREWS AND BOLTS OF DISINTEGRATING SPACECRAFT DURING UNCONTROLLED RE-ENTRY

G. Koppenwallner, B. Fritsche, T. Lips

*HTG Hyperschall-Technologie Göttingen, Max-Planck-Str. 19, 37191 Katlenburg-Lindau, Germany
HTG-mail@t-online.de*

ABSTRACT

Spacecraft usually contain large amounts of screws and bolts in order to connect the elements of primary and secondary structure. These connecting parts are mainly made of stainless steel, a material with high melting temperature. The screws are often protected by the external structure against the high aerodynamic heat loads. During the destruction analysis for a re-entering spacecraft (e.g. with a code system like SCARAB) one usually concentrates on the heavy and larger parts of the main spacecraft structure. In order to assess the possible impact risk of the numerous screws and bolts a fast analysis method for these smaller parts seems necessary. HTG is therefore working on a fast analysis method based on the following simplifying assumptions: Flight dynamic based on Allen/Eggers method, heating based on Stanton number for integral heat transfer, infinite heat conduction within the body, averaged thermal data of materials. Based on these assumptions and an adequate non-dimensional analysis of the different process parameter general rules for the survivability can be deduced.

NOMENCLATURE

A_{ref} Reference area	A_s Surface area
B Ballistic coefficient	c_D Drag coefficient
c_M Moment coefficient	c_p Specific heat capacity
C_s Shape factor	d Diameter
E_{kin} Kinetic energy	Fo Fourier number
h Altitude	h' Scale altitude
h_E Entry altitude	J Moment of inertia
k Thermal conductivity	Kn Knudsen number
L Characteristic length	l Length
m Mass	m_E Entry mass
m_i Ground impact mass	M_A Aerodynamic moment
Ma Mach number	q Dynamic pressure
\dot{q} Heat flux density	q_m Heat of melting
\dot{Q} Heat flux	r_n Nose radius
Re Reynolds number	ST Stanton number
t Time	T_E Entry temperature
T_m Melting temperature	$T_{r,e}$ Radiative equilibrium Temperature
v Velocity	
v_E Entry velocity	V Volume

γ Specific heat ratio	ϵ Emission coefficient
ρ Density	ρ' Reference density
ρ_M Material density	σ Stefan-Boltzmann constant
θ_E Entry angle	λ' Ground mean free path
λ Mean free path	
μ viscosity	
ω Angular acceleration	

Subscripts

C Continuum	FM Free molecular
---------------	---------------------

1. INTRODUCTION

Spacecraft contain large amounts of screws and bolts as fasteners of the different construction elements. These small sized parts are mainly made of stainless steel a material with high melting temperature. These screws are often protected by the external structure against the high aerodynamic heat loads. During the destruction analysis of for a re-entering spacecraft (e.g. with a code system like SCARAB [1]-[4]) one usually concentrates on the heavy and larger parts of the main spacecraft structure. In order to assess the possible impact risk of the numerous screws and bolts a fast analysis method for these smaller parts seems necessary. Due to the small object size scale effects have been considered in the analysis. The scale effects allow on the one side simplified assumption on the other side the rarefied transitional flow regime has to be considered. In the frame of this study we therefore consider in also the influence of regimes with rarefied flow on the object destruction. Our methods thus extend the analytic destruction prediction based on hypersonic laminar continuum heating, e.g. Baker et al. [5] to smaller objects and higher altitudes.

Similar to Baker we rely on the simplified entry dynamics of Allen/Eggers [6]. They assume a straight entry flight path in an exponential isothermal atmosphere (see Fig. 1) with density described by

$$\rho(h) = \rho' \cdot e^{-h/h'} \quad (1)$$

with $\rho' = 1.39 \text{ kg/m}^3$ and $h' = 7162.9 \text{ m}$.

For constant ballistic coefficient B (see Eq. 5) the following solution for the velocity along the re-entry trajectory has been derived:

$$v(h) = v_E \cdot e^{\frac{\rho' h'}{2B \sin \theta_E}} \cdot e^{-\frac{h}{h'}} \quad (2)$$

This solution allows to determine the relevant fluid dynamic parameters like Mach and Reynolds number and heating rate along the trajectory.

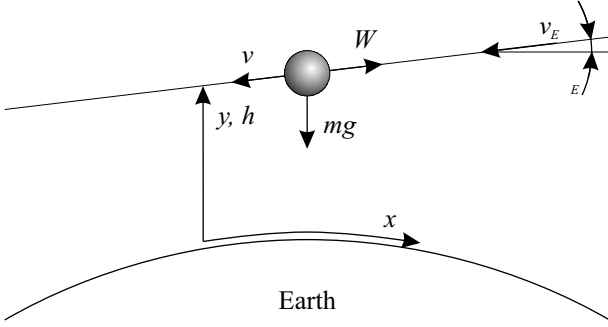


Figure 1. Re-Entry Allen/Eggers [6]

2. SCALE EFFECTS DUE TO SMALL SIZE

The reduction of the size of an object under geometric similarity will not change the general shape of the object. It will however change certain object properties, the reaction of the object on external inputs and the interaction of the object with its surrounding. We consider first the following object quantities and how they change with the characteristic length L .

2.1. Surface Area and Volume

The following dependence exists: Surface area $A_s \propto L^2$, Volume $V \propto L^3$. We thus obtain: $A_s/V \propto 1/L$. This means that with decreasing size the surface area to volume ratio of a body increases with the inverse of the body size.

2.2. Thermal Response Time of a Body to Heat Input

The Fourier number Fo is the natural time scale for unsteady heat conduction resulting e.g. from heat pulses acting on a body of size L .

$$Fo = \frac{kt}{c_p \rho_M L^2} \quad (3)$$

For $Fo > 1$ a heat pulse is in generally penetrated from the body surface to the body center. Thus the characteristic heat penetration time $t_{Fo=1}$ is given by:

$$t_{Fo=1} = \frac{c_p \rho_M L^2}{k} \quad (4)$$

If this time $t_{Fo=1}$ is shorter than the characteristic time t for heat input changes the thermal response of the body may be treated by infinite heat conductivity assumption.

2.3. Ballistic Coefficient or Ratio of Inertia to Aerodynamic Forces

The ballistic coefficient B is defined as

$$B = \frac{m}{c_D A_{ref}} = \frac{\rho_M V}{c_D A_{ref}} \quad (5)$$

As the reference area A_{ref} is like the surface area also proportional to L^2 we obtain $B \propto L$.

2.4. Ratio of Moment of Inertia to Aerodynamic Moments and Angular Acceleration

To calculate the complete dynamic the ratio of moment of inertia to aerodynamic moments is important:

$$\frac{J}{M_A} \approx \frac{\rho_M V L^2}{q c_M A_{ref} L} \quad (6)$$

Eq. 6 leads to $J/M_A \propto L^2$ and for the angular acceleration follows $\omega \propto 1/L^2$. As the moment of inertia decreases with size much faster than the aerodynamic moments the tumbling motion of small bodies will be extremely fast when compared to a large body. This has a strong impact on the analytical numerical tools to treat small body re-entry. Numerical 6-D flight dynamic methods need extremely long time to follow the body on its trajectory. Thus simplified analytical flight dynamics methods seem more appropriate. Fast tumbling exposes the local body surfaces to an average heat load and thus assists the simplified uniform heating assumption.

2.5. Entry Altitude and Flow Regimes

We can define a characteristic ballistic entry altitude given by the altitude $h_{\dot{q}_{max}}$ of maximum laminar heating:

$$h_{\dot{q}_{max}} = h' \cdot \ln \frac{\rho' h'}{B \sin \theta_E} \quad (7)$$

Thus with decreasing L the entry altitude is shifted up to regions of smaller densities.

The main aerodynamic similarity parameters are Mach, Reynolds and Knudsen number. Only Reynolds and Knudsen number, Re and Kn , depend on body size.

$$Re = \frac{\rho v L}{\mu} \quad (8)$$

$$Kn = \frac{\lambda}{L} = 1.26 \sqrt{\gamma} \frac{Ma}{Re} \quad (9)$$

We define 3 flow regimes with the following simple criteria:

- Free molecular flow: $Kn > 10$
- Rarefied transitional flow: $10 > Kn > 0.01$
- Hypersonic continuum flow: $0.01 > Kn$

If we define a characteristic entry Knudsen number at the heat peak heating altitude $h_{\dot{q}_{max}}$ we obtain with mean free path $\lambda(h) = \lambda' \cdot e^{h/h'}$ in exponential atmosphere:

$$Kn_{\dot{q}_{max}} = \frac{\lambda'}{L} \frac{\rho' h'}{B \sin \theta_E} \quad (10)$$

Due to the shift of entry altitude with decreasing body length we obtain now a second power dependence of the Knudsen number on L : $Kn_{\dot{q}_{max}} \propto L^2$.

Fig. 2 shows in an altitude diameter chart the boundaries for the different flow regimes given by corresponding Knudsen numbers. The figure also contains the altitude for maximum heating $h_{\dot{q}_{max}}$ for a sphere as function of diameter. The decelerating entry spreads above and below this maximum heating condition with $\Delta h = 2.81h'$ for deceleration start with $v/v_E = 0.99$, and $\Delta h = -2.63h'$ for the end of the deceleration phase with $v/v_E = 0.1$.

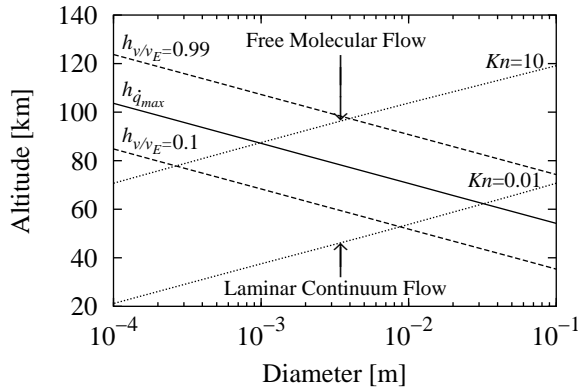


Figure 2. Flow Regimes as Function of Diameter and Altitude of maximum Heating (Sphere, St. Steel, $\theta_E = 2.5^\circ$, $c_D = 1.5$)

3. HEATING LAWS FOR HIGH ALTITUDE/LOW REYNOLDS NUMBER RE-ENTRY

The following simplified definition for Stanton number ST is used:

$$ST = \frac{\dot{Q}}{\rho_\infty / 2 \cdot v_\infty^3 \cdot A_{ref}} \quad (11)$$

The Stanton number in free molecular flow has a constant value of 1.0 independent of the body shape. In the continuum flow regime it depends on the Reynolds number

behind the shock Re_2 and the body shape. According to Lees' theory [7] and experimental data [8], [9] the Stanton number of a sphere can be calculated with Eq. 13.

$$ST_{FM} = 1.0 \quad (12)$$

$$ST_C = 2.1 / \sqrt{Re_2} \quad (13)$$

In order to calculate the Stanton number for other body shapes a shape parameter C_s is used. The shape parameter of a sphere equals 1, the value of C_s of a disk or cylinder equals $1/\sqrt{2}$.

$$ST_C = C_s \cdot 2.1 / \sqrt{Re_2} \quad (14)$$

In the rarefied transition flow regime a bridging formula is used, see Eq. 15 and Fig. 3.

$$ST = \frac{ST_C}{\sqrt{1 + (ST_C/ST_{FM})^2}} \quad (15)$$

The NASA ORSAT code uses a bridging based on an exponential approach [11].

For the relation between Reynolds number behind the shock Re_2 and Knudsen number Kn_∞ we assume Eq. 16. This is a simplification result derived from using a hard sphere gas viscosity law and $\gamma = 1.4$.

$$Kn_\infty = \frac{3.33}{Re_2} \quad (16)$$

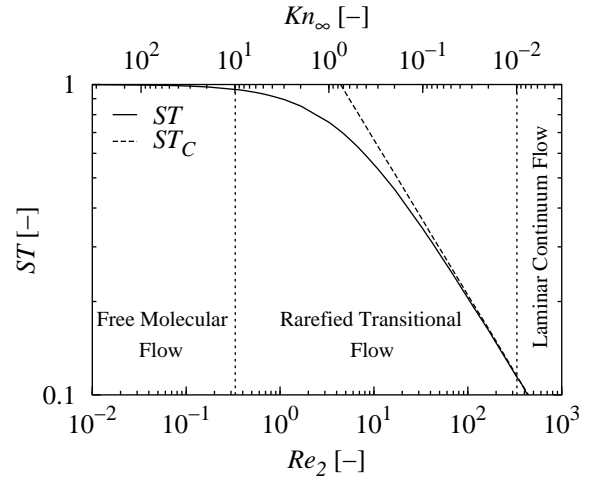


Figure 3. Stanton Number vs. Reynolds and Knudsen Number

4. MATERIAL PROPERTIES

In the frame of this study 5 materials were considered: Titanium (TiAl6V4), Stainless Steel (A316), Inconel, Aluminum (AA7075) and Copper. The material properties

are listed in Tab. 1. The temperature depending properties heat capacity c_p , thermal conductivity k and emission coefficient ϵ were averaged over temperature from 300 K to melting temperature. As data sources served [13], [14].

Fig. 4 shows a comparison of the total specific heat absorption capacities of these materials including the specific heat needed to increase the temperature from 300 K to melting temperature plus specific heat of melting q_m . This sum is the total amount of specific heat a material can stand until it is molten completely. This shows that Titanium is the most likely material to survive re-entry and therefore the most critical, followed by stainless steel.

Table 1. Material Properties

Material	ρ_M [kg/m ³]	c_p [J/kgK]	ϵ [%]	T_m [K]	q_m [J/g]
Titanium	4420	750.0	30.2	1900	400
St. Steel	8030	611.5	35.0	1650	274
Inconel	8190	417.1	12.2	1570	309
Aluminum	2800	751.1	14.1	870	385
Copper	8960	434.1	21.6 ^a	1356	243

^aoxidized; polished: $\epsilon = 1.2\%$

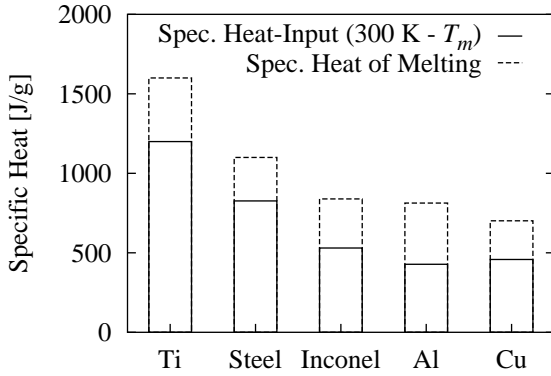


Figure 4. Total Specific Heat Absorption Capacities of different Materials

5. COMBINED AERO-THERMAL AND FLIGHT DYNAMIC FORMULATION

Analytic formulations for hypersonic heating combined with re-entry dynamics have been derived already before the early stages of space flight. Classical contributions are the studies of Allen/Eggers [6] and Chapman [12]. They in principle used a simple but quite realistic exponential atmosphere model in combination with ballistic entry dynamics and laminar stagnation point heat transfer laws.

5.1. Energy Balance during Aero-Braking

A basic understanding of the connection between aero-heating and aero-braking can be obtained of simple momentum end energy balance equations for a body.

Momentum equation:

$$m \frac{dv}{dt} = -\frac{1}{2} \rho v^2 c_D A_{ref} \quad (17)$$

Heat transferred to the body:

$$\frac{dQ}{dt} = \frac{1}{2} ST \rho v^3 A_{ref} \quad (18)$$

Combining Eq. 17 and 18 we obtain:

$$dQ = -\frac{ST}{c_D} m v dv = -\frac{ST}{c_D} dE_{kin} \quad (19)$$

With $E_{kin} = m/2 \cdot v^2$ the kinetic energy of the complete entry body.

For constant values of Stanton number ST and drag coefficient c_D , which is only in free molecular conditions true ($ST = 1$ and $c_D = 2$) we can integrate the above equation and obtain for a velocity reduction from $v = v_E$ to $v = 0$

$$\frac{Q}{m} = -\frac{1}{2} \frac{ST}{c_D} v_E^2 \quad (20)$$

Q/m represents the heat transferred to the body per unit mass and $1/2 \cdot v^2$ the mass specific kinetic initial energy of the body. ST/c_D can have a maximum value at free molecular flow conditions of 0.5. Thus in the extreme case 1/4 of the objects kinetic energy can be transferred as heat to the body.

5.2. Energy Balance for Body Heating and Melting

We allow aerodynamic and radiative interaction of the body with its ambient. We obtain then the following heat flux balance for a body with infinite heat conduction.

Body before melting $T < T_m$:

$$\rho_M V c_p \frac{dT}{dt} + \epsilon \sigma A_S T^4 = \dot{Q}_{aero}(t) \quad (21)$$

Body during melting process $T = T_m$:

$$-\rho_M q_m \frac{dV}{dt} + \epsilon \sigma A_S T_m^4 = \dot{Q}_{aero}(t) \quad (22)$$

For $T = T_m$ melting starts which has been defined as failure event and body volume reaching $V = 0$ the body demise event occurs [5].

Concerning the thermal body response we can discriminate 2 extreme cases:

- No radiative heat loss $dT/dt \propto \dot{Q}_{aero}(t)$
- No heat storage capacity $T(t) = T_{r,e}(t)$

Case b. defines the radiative equilibrium temperature $T_{r,e}$.

5.3. Analytic Expressions for Heating along Trajectory

For the continuum laminar and free molecular heating the following expressions can be derived:

Continuum laminar heating:

$$\dot{Q}_{aero}(h) = \frac{\rho(h)}{2} v^3(h) \frac{2.1}{\sqrt{Re_2}} C_s A_{ref} \quad (23)$$

Free molecular heating:

$$\dot{Q}_{aero}(h) = \frac{\rho(h)}{2} v^3(h) A_{ref} \quad (24)$$

For the maximum heat peak heating rates the following expressions can be derived:

Laminar flow:

$$\begin{aligned} \dot{Q}_{max} &= C_{lam} \sqrt{\frac{1}{3eh'}} \sqrt{\frac{B \sin \theta_E}{r_n}} v_E^3 C_s A_{ref} \quad (25) \\ C_{lam} &= 1.23 \cdot 10^{-4} \text{ kg}^{0.5} \text{ m}^{-1} \end{aligned}$$

occurring at $v/v_E = e^{-1/6}$ and $h = h' \ln\left(\frac{3\rho'h}{B \sin \theta_E}\right)$.

Free molecular flow:

$$\dot{Q}_{max} = \frac{1}{3e} \left(\frac{B \sin \theta_E}{\rho' h'} \right) \rho' v_E^3 A_{ref} \quad (26)$$

occurring at $v/v_E = e^{-1/3}$ and $h = h' \ln\left(\frac{3}{2} \frac{\rho' h}{B \sin \theta_E}\right)$.

5.4. Simple Analytic Failure Event Criteria

For large bodies with laminar heating during re-entry such criteria have been already derived by Baker [5]. This criteria can not be applied to small bodies with transitional or free molecular heating, because the laminar heating law over predicts for $Kn > 1$ the aerodynamic heating.

A simple criteria for failure can be established if we compare the radiative equilibrium temperature $T_{r,e}$ at peak heating with the melting temperature of body material T_m . Thus failure (melting) will occur for $T_m \leq T_{r,e}$ because the body is not able to radiate the peak heat flow into surrounding.

For spherical bodies and laminar continuum heating the following failure criteria can be derived:

$$T_m^4 \frac{\epsilon}{\sqrt{\rho_M}} \leq C_{lam} \sqrt{\frac{4}{9eh'}} \sqrt{\frac{\sin \theta_E}{c_D}} \frac{1}{4\sigma} v_E^3 \quad (27)$$

It turns out that this criteria is independent of body size and only dependent on the material properties.

For molecular heating we obtain:

$$T_m^4 \frac{\epsilon}{\rho_M} \frac{1}{d} \leq \frac{1}{18eh'} \frac{\sin \theta_E}{\sigma c_D} v_E^3 \quad (28)$$

In this case the criteria depends both on body size and on the material properties. With decreasing diameter d also the failure event is reduced. Thus smaller particle are more likely to survive.

The last equation allows to directly determine the failure diameter d_F of spherical objects:

$$d_F = 18eh' \frac{c_D}{\sin \theta_E} \frac{1}{v_E^3} \frac{\epsilon \sigma}{\rho_M} T_m^4 \quad (29)$$

In the expressions above we have grouped influence factors according to their origin e.g. properties of body material, entry flight conditions. Concerning the survivability the following combination of body properties are important: $T_m^4 \frac{\epsilon}{\sqrt{\rho_M}}$ for laminar heating, $T_m^4 \frac{\epsilon}{\rho_M} \frac{1}{d}$ for free molecular heating.

6. NUMERICAL ANALYSIS RESULTS AND ANALYTIC PREDICTION

In the numerical integration methods the following special features were used: Heat transfer law covering the transition from free molecular to laminar continuum flow as described in chapter 3, U.S. Standard Atmosphere 1976 [15] to calculate atmosphere temperature (and therefrom temperature dependent physical data like mean free path λ and viscosity μ). The numerical integration itself is a simple Euler's method with fixed altitude step size. Time steps are calculated from actual velocity, altitude step size and flight path angle.

For our calculations the following re-entry conditions were used: $h_E = 200$ km, $v_E = 7.8$ km/s, $\theta_E = 2.5^\circ$ and $T_E = 300$ K.

The results were calculated for 3 different body shapes (sphere, cylinder and disk) consisting of the materials described in chapter 4. In Fig. 5 - 7 the demise altitude is plotted vs. the diameter of the re-entering object. It can be seen that there exists an upper and a lower critical diameter. This means that smaller respectively bigger objects always reach ground.

As mentioned above Titanium is the most critical material. It has the smallest diameter range in which demise occurs. Therefore Fig. 8 shows the demise altitude only for titanium spheres, disks and cylinders.

In order to determine a ground risk from surviving objects the ground impact mass is important. Fig. 9 shows the relative impact mass m_i/m_E . These results are not completely realistic because a 5 cm Titanium sphere will not reach ground without any part of it molten. Here our assumption of infinite thermal conductivity is not valid anymore.

With Eq. 29 the minimum failure diameters of spheres were calculated. They are in good agreement with the numerical results (see Tab. 2).

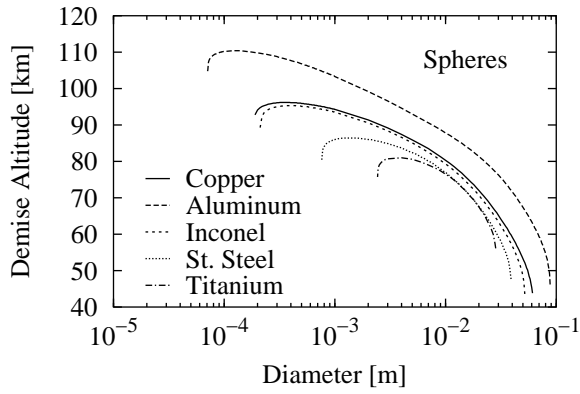


Figure 5. Demise Altitude of Spheres

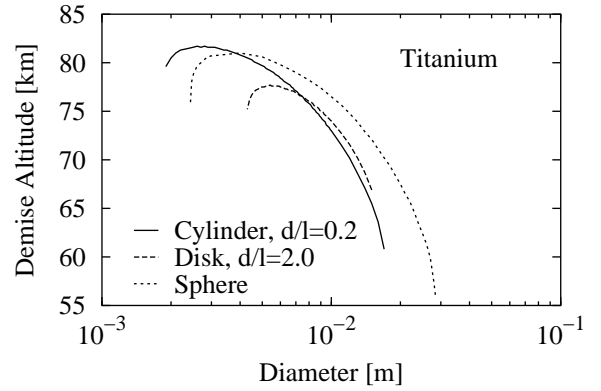


Figure 8. Demise Altitude of Titanium for different Shapes

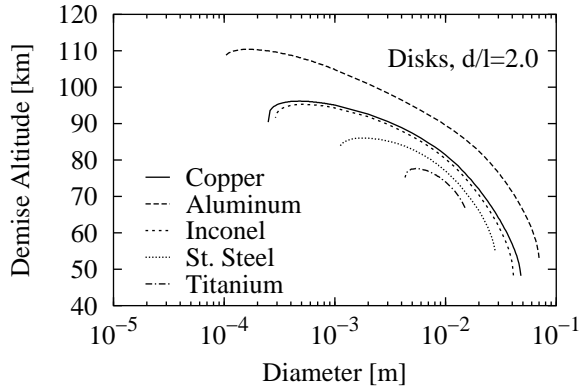


Figure 6. Demise Altitude of Disks

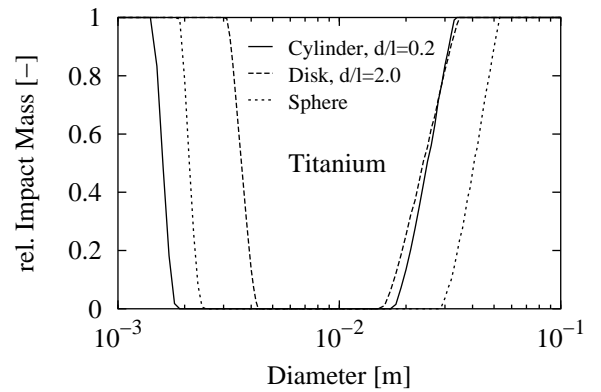


Figure 9. Relative Ground Impact Mass m_i/m_E of Titanium for different Shapes

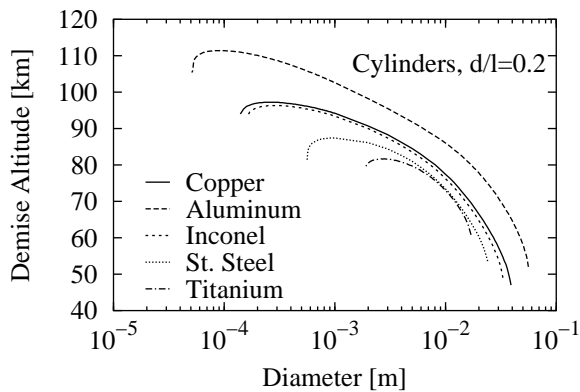


Figure 7. Demise Altitude of Cylinders

Table 2. Comparison of Analytical and Numerical Minimum Failure Diameters of Spheres (Free Molecular Heating)

Material	analytical numerical	
	d_F [mm]	
Titanium	1.71	2.43
St. Steel	0.62	0.76
Inconel	0.17	0.21
Aluminum	0.05	0.07
Copper	0.15	0.19

7. CONCLUSION

Simple analytical and fast numerical integration methods for survivability analysis of small debris objects have been developed.

Small objects decelerate at high altitudes and therefore flow rarefaction effects have to be considered in heating law. Laminar continuum heating would in this case strongly over predict the heating.

3 solid object shapes (sphere, disc, cylinder) and 5 materials have been used to test the methods.

Our analysis showed that for each material and each shape there exist the following two boundaries for surviving at minimum partially the re-entry from orbit.

Minimum size limit: This limit is due to high altitude re-entry with free molecular heating. Re-radiation of the aero-heating allows the bodies to survive the re-entry.

Maximum size limit: This limit occurs in the laminar heating regime for larger solid objects. Re-radiation and heat storage allow the bodies to survive.

Open points for further investigations are: Influence of finite heat conductivity on survivability analysis, survivability dependence on exposure altitude and velocity.

REFERENCES

1. Fritsche B. et al., *Spacecraft disintegration during uncontrolled atmospheric Re-entry*, Executive Summary ESOC Contract No. 11427/95/D/IM, Katlenburg-Lindau, Germany, 1997.
2. Fritsche B. et al., *Spacecraft disintegration during uncontrolled atmospheric Re-entry*, IAA-99-IAA.6.7.02, 50th Int. Astronautical congress, Amsterdam, 1999.
3. Fritsche B. et al., *Advanced Model for Spacecraft Disintegration during Atmospheric Re-entry*, Executive Summary ESOC Contract 12804/98/D/IM, HTG Report 00-04, Katlenburg-Lindau, Germany, 2000.
4. Klinkrad H., Fritsche B., *Thermal Destruction of Hollow Spheres during Atmospheric Entry*, Test Results Computed with the SCARAB S/W System, 16th IADC meeting, Toulouse, 1998.
5. Baker R.L. et al., *Orbital spacecraft Re-entry Breakup*, IAA-99-IAA.6.7.04, 50th Int. Astronautical Congress, Amsterdam, 1999.
6. Allen H. J., Eggers jr. A. J., *A study of the motion and aerodynamic Heating of Missiles entering the Earth's Atmosphere at High Supersonic Speeds*, NACA TN-4047, Washington, 1957.
7. Lees L., *Laminar Heat Transfer over Blunt Nosed Bodies at Hypersonic Speeds*, Jet Propulsion Vol. 26, No. 4, pp.259-269, 1956.
8. Koppenwallner G., *Rarefied Gas Dynamics in Hypersonics Volume 1*, Defining Hypersonic Environment Ed. Bertin et al., Birkhuser, Boston, Basel, Berlin, 1989.
9. Koppenwallner G., *Aerothermodynamic behavior of NPS during Re-entry*, IB 222-88 A 05, DFVLR, Göttingen 1987.
10. Rochelle W. et al., *Modeling of Space Debris Re-entry Survivability and Comparison of Analytical Methods*, IAA-99-IAA.6.7.03, 50th Int. Astronautical Congress, Amsterdam, 1999.
11. Anonym, *Users Guide for Object Re-entry Survival Analysis Tool (ORSAT)- Version 5*, NASA, Lyndon B. Johnson Space Center, LMSEAT-33175, Houston, Texas, 1999.
12. Chapman D. R., *An Approximate Analytical Method for Studying Entry into Planetary Atmospheres*, NACA TN-4276, Washington, 1958.
13. Landolt-Brnstein, *Zahlenwerte und Funktionen aus Physik, Chemie, Astronomie, Geophysik, Technik*, IV. Band, 2. Teil, 6. Auflage, Springer-Verlag, Berlin, 1963/64
14. Goldsmith A., Hirschhorn H. J., Waterman T. E., *Thermophysical Properties of Solid Materials*, Volume II - Alloys, Armour Research Foundation, WADC TR 58-476, 1960
15. *U.S. Standard Atmosphere, 1976*, National Oceanic and Atmosphere Administration, National Aeronautics and Space Administration, Washington D.C., 1976.